第 27 卷第 12 期 无 机 化 学 学 报 Vol.27 No.12
2011 年 12 月 CHINESE JOURNAL OF INORGANIC CHEMISTRY 2494-2500

两种甲氧基苯基咔咯铜配合物的合成及光谱性质

朱卫华 陈 晨 房媛媛 练翠翠 路桂芬 欧忠平*
(江苏大学化学化工学院,镇江 212013)

摘要:合成了两个中位苯基上具有甲氧基取代基的铜咔咯配合物(T*p*-OCH_3PC)Cu 和(T*o*,*p*-$(OCH_3)_2$PC)Cu,通过紫外-可见、红外光谱、元素分析、核磁共振及质谱对它们进行了表征。研究了配合物在非水溶剂中的电子顺磁共振、电化学和光谱电化学性质,结果表明无论在固体状态还是在非水溶剂中,配合物的中心金属离子均为三价铜 Cu(Ⅲ),在给定的溶剂中 Cu(Ⅲ)可以发生可逆的还原反应生成 Cu(Ⅱ),也可以被可逆氧化为 Cu(Ⅲ)的阳离子自由基。探讨了甲氧基取代基以及溶剂对配合物的紫外-可见光谱和氧化还原电位的影响。

关键词:铜咔咯;合成;表征;电化学;光谱性质
中图分类号:O641.121 **文献标识码**:A **文章编号**:1001-4961(2011)12-2494-07

Synthesis and Spectral Properties of Two Copper Methoxyphenylcorrole Complexes

ZHU Wei-Hua CHEN Chen FANG Yuan-Yuan LIAN Cui-Cui LU Gui-Fen OU Zhong-Ping*
(*School of Chemistry and Chemical Engineering, Jiangsu University, Zhenjiang, Jiangsu* 212013, *China*)

Abstract: Two copper methoxyphenylcorrole complexes were synthesized and characterized by UV-Vis, FTIR, ^{1}H NMR, MS and ESR spectroscopies. The investigated corroles are represented as (T*p*-OCH_3PC)Cu and (T*o*,*p*-$(OCH_3)_2$PC)Cu, where T*p*-OCH_3PC and T*o*,*p*-$(OCH_3)_2$PC are the trianion of the 5,10,15-tri(4-methoxyphenyl)corrole and 5,10,15-tri(2,4-dimethoxyphenyl)corrole, respectively. Neutral copper complexes expected to contain the low spin d^8 Cu(Ⅲ) central ions exhibit no ESR signal in the solid state and in CH_2Cl_2 or DMF solutions, thin-layer UV-Visible spectroelectrochemistry result indicates that the first reduction of Cu(Ⅲ) corroles leads to formation of a Cu(Ⅱ) species in non-aqueous media while the first oxidation of the same compound is corrole ring-centered to give a Cu(Ⅲ) π-cation radical under the same solution conditions. Effects of the electron-donating OCH_3 substituents and the solvent on the UV-Vis spectra and redox potentials of the copper corrole were discussed.

Key words: copper(Ⅲ) corrole; synthesis; characterization; electrochemistry; spectral property

Metallocorroles have attracted more and more interests in the past decades[1-6], in part because the facile synthesis methods have been available for these compounds[4-6] and in part because they have been shown a number of promising applications in the fields of catalysis, sensors and photodynamic therapy[3,4,7-11].

A variety of transition metals, such as Cr, Mn, Fe, Co, Ag, Cu, Zn, Ru, Rh, Ni or Pd and the main group elements As, Sb, P, Al, Ga or Sn, have been used as central ions for the synthesis of metallocorroles[4-6]. Among them, the copper was often utilized because it is easy to insert into the corrole macrocycle to produce a four-coordinate copper corrole complex. Therefore, a number of copper corroles have been synthesized and

收稿日期:2011-09-30。收修改稿日期:2011-10-14。
国家自然科学基金(No.21071067,21001054)资助项目。
*通讯联系人。E-mail:zpou2005@yahoo.com.cn,Fax:086-0511-88791800

characterized in recent years[12-22].

Synthesis and study of substituted copper corroles are a part of our recent research interests[12-13,19,23]. In the present paper, two copper corroles containing OCH_3 groups on the meso-phenyl rings of the corrole macrocycle were synthesized and characterized. The compounds are represented as (T*p*-OCH_3PC)Cu and (T*o*,*p*-$(OCH_3)_2$PC)Cu, where T*p*-OCH_3PC and T*o*,*p*-$(OCH_3)_2$PC are the trianion of the 5,10,15-tris(4-methoxyphenyl)corrole and 5,10,15-tris(2,4-dimethoxyphenyl)corrole, respectively. ESR, UV-Vis spectral and spectroelectrochemical properties for each copper corrole were examined in non-aqueous media. Neutral copper complexes in the solid state and in a solution of CH_2Cl_2 or DMF exhibit no ESR signal, which is expected for the corroles containing the low spin d^8 Cu(Ⅲ) central ions. Thin-layer UV-Visible spectroelectrochemistry and ESR measurements indicate that the first reduction of each copper corrole is metal-centered and leads to the formation of a Cu(Ⅱ) species while the first oxidation is corrole ring-centered to give a Cu(Ⅲ) π-cation radical in CH_2Cl_2 and DMF containing 0.1 mol·L^{-1} TBAP. The effects of the electron-donating OCH_3 substituents and the solvent on the UV-Visible spectra and redox potentials of the copper corrole were also discussed.

1 Experimental

1.1 Instrumentation

^{1}H NMR spectra were recorded in a $CDCl_3$ solution at 400 MHz using a Bruker Advance 400 spectrometer at 25 ℃. Chemical shifts (ppm) were determined with TMS as the internal reference. ESR spectra were recorded on a Bruker 300C spectrometer. Elemental analyses were obtained from the EA1112 and infrared spectra were recorded with Nicolet Nexus 470. MALDI-TOF mass spectra were carried out on a Bruker BIFLEX Ⅲ ultrahigh resolution. Cyclic voltammetry was carried out by using CHI730C Electrochemical Workstation or an EG&G Princeton Applied Research (PAR) 173 potentiostat/galvanostat. A home-made three-electrode cell (a glassy carbon working electrode, a platinum counter electrode and a homemade saturated calomel reference electrode (SCE)) was used for cyclic voltammetric measurements. The SCE was separated from the bulk of the solution containing the solvent/supporting electrolyte mixture by a fritted glass bridge of low porosity.

Thin-layer UV-Visible spectroelectrochemical experiments were performed with a home-built thin-layer cell with a light transparent platinum net working electrode. Potentials were applied and monitored with an EG&G PAR Model 173 potentiostat. Time-resolved UV-Visible spectra were recorded with a Hewlett-Packard Model 8453 diode array spectrophotometer. High purity N_2 was used to deoxygenate the solution and kept over the solution during each electrochemical and spectroelectrochemical experiment.

A part of electrochemistry, spectroelectrochemistry and ESR experiments were carried out in Dr. Kadish′s lab in Houston, USA.

1.2 Chemicals

Reagents and solvents (Sigma-Aldrich, Fluka or Sinopharm Chemical Reagent Co.) for synthesis and purification were of analytical grade and used as received. N,N-dimethylformamide (DMF, +99.8%) and pyridine (+99.9%) were purchased from Sigma-Aldrich and used as received. Dichloromethane (CH_2Cl_2, +99.8%) was purchased from EMD Chemicals Inc. and used as received. Tetra-*n*-butylammonium perchlorate (TBAP) was purchased from Sigma Chemical or Fluka Chemika Co. and used as received.

1.3 Synthesis of copper corroles

The free-base corroles, (T*p*-OCH_3PC)H_3 and (T*o*,*p*-$(OCH_3)_2$PC)H_3, were synthesized and purified according to the procedure previously described[24].

(T*p*-OCH_3PC)Cu. The free-base corrole (T*p*-OCH_3PC)H_3 (0.050 g, 0.08 mmol) was dissolved in 10 mL of pyridine at room temperature. After degassed by bubbling nitrogen for 5 min, 0.055 g (0.28 mmol) copper acetate monohydrate was added into the solution. The mixture was stirred for 30 min. The progress of the reaction was followed up by absorption spectroscopy. The pyridine was removed via vacuum distillation and the pure product was obtained by flash chromatography of the residue on silica gel with CH_2Cl_2

as eluent in 93% yield. ^{1}H NMR (400 MHz; $CDCl_3$): δ, ppm 3.95 (s, 9H), 7.02~7.06 (m, 7H), 7.37~7.40 (d, 4H), 7.68~7.73 (t, 4H), 7.79 (d, 3H), 7.91 (s, 2H). IR (KBr): ν, cm^{-1} 2 926, 2 832, 1 597, 1 506, 1 422, 971, 813, 700. MS (MALDI-TOF): 677.13 (M^+); calcd. 677.15. Anal. calcd. for $C_{40}H_{29}N_4O_3Cu$: C, 70.94; H, 4.32; N, 8.27%. Found: C, 70.11; H, 4.12; N, 8.06%.

(T*o*,*p*-$(OCH_3)_2$PC)Cu. The free-base corrole (T*o*,*p*-$(OCH_3)_2$PC)H_3 (0.050 g, 0.07 mmol) was dissolved in 10 mL of degassed pyridine at room temperature, 0.055 g (0.28 mmol) copper acetate monohydrate was added. Then the same procedure as described above for the synthesis and purification of (T*p*-OCH_3PC)Cu was utilized and a pure product was obtained in a yield of 90%. ^{1}H NMR (400 MHz; $CDCl_3$): δ, ppm 3.72~3.94 (d, 18H), 6.65 (m, 6H), 7.10 (m, 3H), 7.48 (m, 5H), 7.93 (m, 3H). IR (KBr): ν, cm^{-1} 2 917, 2 843, 1 674, 1 605, 1 576, 1 503, 1 454, 1 298, 1 204, 1 160, 1 021, 792. MALDI-TOF-MS: 767.10 (M^+); calcd. 767.18. Anal. calcd. for $C_{43}H_{35}N_4O_6Cu$: C, 67.31; H, 4.60; N, 7.30%. Found: C, 67.21; H, 4.51; N, 7.18%.

2 Results and discussion

2.1 Synthesis

(T*p*-OCH_3PC)Cu and (T*o*,*p*-$(OCH_3)_2$PC)Cu were synthesized in pyridine at room temperature (Scheme 1). The insertion of copper is a facile process for both compounds, proceeding to completion within 30 min. The pure dark green complexes are obtained in high yield and confirmed with ^{1}H NMR spectra, through the absence of an inner NH resonance, the metal (Ⅲ) chelation has taken place. High resolution mass spectrum exhibits a molecular peak at *m*/*z* of 677.13 for (T*p*-OCH_3PC)Cu and 767.10 for (T*o*,*p*-$(OCH_3)_2$PC)Cu with no additional major peaks. The data thus are in perfect agreement with the expected molecular formula of the copper corroles.

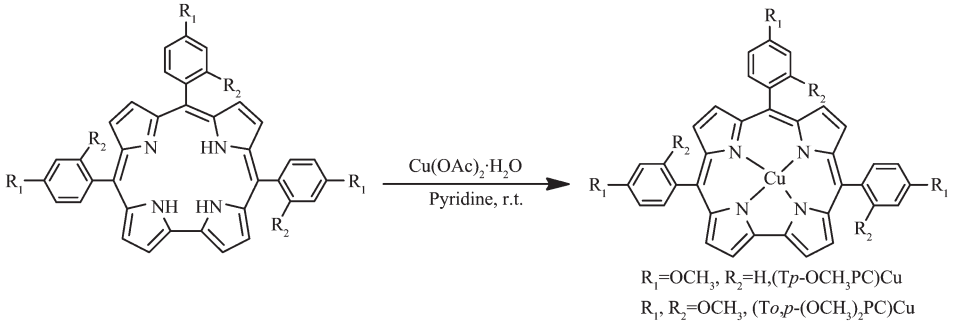

Scheme 1 Synthesis route for copper corroles

2.2 Electronic absorption spectra

Electronic absorption spectra of copper corroles were measured in CH_2Cl_2, PhCN, DMF and pyridine. Similar UV-Visible spectra were observed for each corrole in the four different solvents. The Soret bands are located at 435~437 nm and 437~439 nm for neutral (T*p*-OCH_3PC)Cu^{Ⅲ} and (T*o*,*p*-$(OCH_3)_2$PC)Cu^{Ⅲ}, respectively. The difference of the Soret band maximum is only 1~2 nm in these solvents, indicating no significant effect of the solvent on UV-Visible spectra of the copper corroles.

The electronic absorption spectra of copper corroles are sensitive to the peripheral substituents[23,25]. As seen in Table 1, the electron-donating groups on the meso-phenyl rings of the corrole macrocycle may cause a red-shift of the spectra while the electron-withdrawing groups can lead to a blue-shift under the same solution conditions. Therefore, (T*p*-OCH_3PC)Cu with a OCH_3 group on each of the three meso-phenyl rings of the corrole macrocycle shows absorption at 433 nm in CH_2Cl_2 and has 27 nm red-shift as compared to its parent triphenylcorrole, (TPC)Cu, with no substituents on the meso-phenyl rings. (T*o*,*p*-$(OCH_3)_2$PC)Cu exhibits a Soret band at 439 nm in CH_2Cl_2 consistent with the expected red-shift as compared to (T*p*-OCH_3PC)Cu because a second OCH_3 group is added to the *meso*-phenyl rings of the compound.

The energy (*E*, eV) of the Soret band for the copper

Table 1　Soret band absorption maxima (λ_{max}, nm) and redox potentials (V vs SCE) for copper(Ⅲ) *meso*-triarylcorroles in CH_2Cl_2

Compound	Substituent[a]	$\sum\sigma$	Soret band		Potential / V		ΔE / V[c]	Ref.
			λ_{max} / nm	E / eV[b]	1st ox	1st red		
(TF_5PC)Cu **1**	5F	3.66	406	3.054	1.12	0.21	0.91	[23]
(Tp-CF_3PC)Cu **2**	CF_3	1.65	406	3.054	0.89	−0.06	0.95	[23]
(TPC)Cu **3**	None	0.0	410	3.024	0.78	−0.19	0.97	[23]
(T*p*-CH_3PC)Cu **4**	CH_3	−0.51	416	2.981	0.70	−0.23	0.93	[23]
(T*p*-OCH_3PC)Cu **5**	OCH_3	−0.81	433	2.864	0.64	−0.25	0.89	tw
(T*o*,*p*-$(OCH_3)_2PC$)Cu **6**	$2OCH_3$	−1.98	439	2.825	0.61	−0.27	0.88	tw

[a] Substituents on each *meso*-phenyl ring of the corrole; [b] Energy of the Soret band; [c] Potential difference between the first oxidation and first reduction (HOMO-LUMO gap); tw: this work.

(Ⅲ) corroles in CH_2Cl_2 varies linearly with the electron-donating or electron-withdrawing nature of substituents on the three phenyl rings of the macrocycle. A plot of E vs the sum of the Hammett substituent constants ($\sum\sigma$)[26] is shown in Fig.1a and indicates that the substituents on the meso-phenyl rings have a significant effect on the Soret band of the Cu(Ⅲ) corroles.

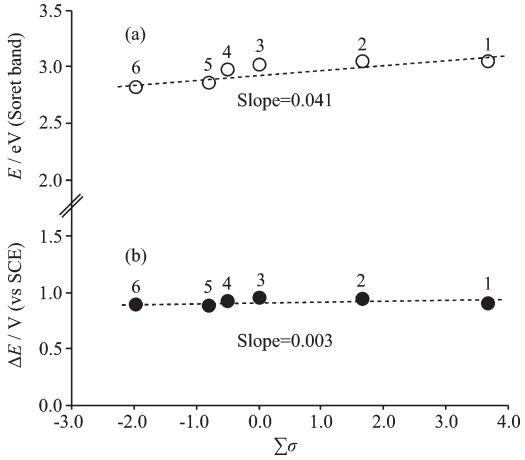

Fig.1　Plots for the energy of Soret band (E / eV) or the HOMO-LUMO gap (ΔE / V) vs the Hammett substituent constant ($\sum\sigma$) of the meso-phenyl substituted copper(Ⅲ) corroles (data taken from Table 1)

2.4　Electrochemistry

The electrochemistry of (T*p*-OCH_3PC)Cu and (T*o*,*p*-$(OCH_3)_2PC$)Cu was carried out in CH_2Cl_2 containing 0.1 mol·L^{-1} TBAP and the half-wave potentials for the first oxidation and first reduction are given in Table 1. As a comparison, the redox potentials for four related *meso*-phenyl substituted Cu(Ⅲ) corroles are also included in the table.

Both copper corroles undergo three oxidations and one reduction between 1.8 and −2.0 V vs SCE. The reduction occurs at $E_{1/2}$=−0.25 V for (T*p*-OCH_3PC)Cu and at −0.27 V for (T*o*,*p*-$(OCH_3)_2PC$)Cu (Table 1) and is assigned as a $Cu^{Ⅲ}/Cu^{Ⅱ}$ process. Similar redox potentials have been reported for other related copper(Ⅲ) triphenylcorroles containing electron-donating or electron-withdrawing substituents on the *meso*-phenyl and/or β-pyrrole positions of the macrocycle. (TPC)Cu is reduced at −0.16 V in CH_2Cl_2 while the formal $Cu^{Ⅲ}/Cu^{Ⅱ}$ process for the other corroles varies from $E_{1/2}$=−0.22 to 0.64 V, depending upon the type and position of the electron-withdrawing or electron-donating substituents[23].

The oxidations were observed at $E_{1/2}$=0.64, 1.28 and 1.58 V for (T*p*-OCH_3PC)Cu and at 0.61, 1.17 and 1.36 V for (T*o*,*p*-$(OCH_3)_2PC$)Cu in CH_2Cl_2. All the three electron abstraction processes are corrole macrocycle-centered electron transfer reactions under the given solution conditions. As seen from Table 1, (T*o*,*p*-$(OCH_3)_2$PC)Cu is harder to reduce and easier to oxidize than (T*p*-OCH_3PC)Cu due to the fact that a second electron-donating group OCH_3 has been added onto each phenyl ring of the corrole macrocycle.

It is worth to point out that the substituent effect on the first reduction is almost the same as on the first oxidation, therefore no big difference is seen for the HOMO-LUMO gap ($\Delta E_{1/2}$) of these copper corroles (see Table 1 and Fig.1b). For example, the $\Delta E_{1/2}$ is equal to 0.91 V for (TF_5PC)Cu with five electron-withdrawing F groups on each of the meso-phenyl ring and almost the same value (0.88 V) is obtained for ((T*o*,*p*-$(OCH_3)_2PC$)

Cu with total six electron-donating OCH_3 substituents on the three phenyl rings of the corrole macrocycle.

One oxidation and two reductions were observed for both copper corroles in DMF, 0.1 mol·L^{-1} TBAP. The redox potentials are located at 0.66, −0.17 and −1.98 V for (T*p*-OCH_3PC)Cu and at 0.62, −0.20 and −2.05 V for ((T*o*,*p*-$(OCH_3)_2$PC)Cu. Like in CH_2Cl_2, the second OCH_3 group also leads to a negative potential shift in DMF upon going from (T*p*-OCH_3PC)Cu to ((T*o*, *p*-$(OCH_3)_2$PC)Cu.

Both copper corroles are easier to reduce in DMF than in CH_2Cl_2. For example, the first reduction potential of Cu^{III}/Cu^{II} process for ((T*o*,*p*-$(OCH_3)_2$PC)Cu is located at $E_{1/2}$ of −0.20 V in DMF, while the same process occurs at −0.27 V in CH_2Cl_2. Thus, a 70 mV positive shift can be seen in $E_{1/2}$ upon going from CH_2Cl_2 to DMF as the solvent (Fig.2). However, the potential of the ring-centered oxidation for the compound only have a 10 mV positive shift as the solvent changing from CH_2Cl_2 to DMF. The results indicate that the strong binding ability of DMF has a significant effect on the reduction and only a weak effect on the oxidation of the copper corroles.

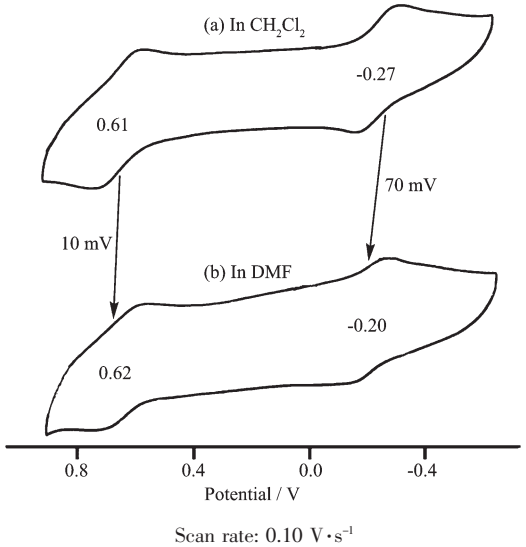

Fig.2 Cyclic voltammograms of (T*o*,*p*-$(OCH_3)_2$PC)Cu in (a) CH_2Cl_2 and (b) DMF containing 0.1 mol·L^{-1} TBAP

2.5 Spectroelectrochemistry

Thin-layer UV-Visible spectroelectrochemical studies for each copper corrole were carried out in CH_2Cl_2 and DMF containing 0.1 mol·L^{-1} TBAP. As an example, the UV-Visible spectral changes of (T*p*-OCH_3PC)Cu during the first and second controlled potential reductions and the first oxidation in DMF are illustrated in Fig.3.

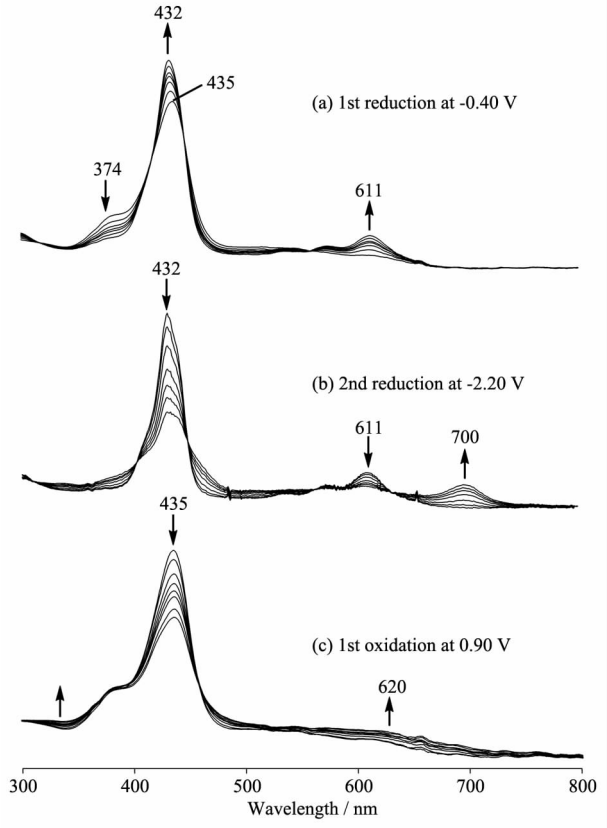

Fig.3 Thin-layer UV-Visible spectral changes of (T*p*-OCH_3PC)Cu obtained during the first two reductions at (a) −0.40 V, (b) −2.20 V and (c) the first oxidation at 0.90 V in DMF containing 0.1 mol·L^{-1} TBAP

The Soret band at 435 nm slightly increases in intensity and shifts to 432 nm, while a new Q band grows in 611 nm upon the first reduction at −0.40 V in DMF. The first reduction is assigned as a metal-centered electron transfer process and leads to the formation of the Cu(Ⅱ) corrole as previously reported for other related cupper corroles[12-13,23]. The neutral corrole could be regenerated when the potential is set back to 0.40 V, indicating that the singly reduced species is stable on the thin-layer spectroelectrochemistry timescale.

During the second reduction of (T*p*-OCH_3PC)Cu at

−2.20 V in DMF the Soret band at 432 nm and Q band at 611 nm both decrease in intensity while a broad absorption band grows up at 700 nm (Fig.3b), indicating that the electrogenerated Cu(Ⅱ) corroles can be further reduced at a more negative potential to give a Cu(Ⅱ) corrole π-anion radical under the given solution conditions. The UV-Visible spectral changes obtained upon the first oxidation of (T*p*-OCH_3PC)Cu (Fig.3c) are consistent with a Cu(Ⅲ) π-cation radical generated from the initial Cu(Ⅲ) complex in DMF containing 0.1 mol·L^{-1} TBAP.

Similar spectral changes are also seen for (T*o*,*p*-$(OCH_3)_2$PC)Cu upon the stepwise controlled potential reductions and oxidation in a thin-layer cell, indicating the same type of products are generated as that of (T*p*-OCH_3PC)Cu, i.e. [(T*o*,*p*-$(OCH_3)_2$PC)$Cu^{Ⅱ}$]$^-$ and [(T*o*,*p*-$(OCH_3)_2$PC)$Cu^{Ⅱ}$]$^{2-}$ are formed upon the first two one-electron reductions, and [(T*o*,*p*-$(OCH_3)_2$PC)$Cu^{Ⅲ}$]$^+$ is produced upon the first one-electron oxidation under the same solution conditions.

2.3 ESR characterization

ESR measurements of (T*p*-OCH_3PC)Cu and (T*o*,*p*-$(OCH_3)_2$PC)Cu were carried out in a solid state and in the solution of CH_2Cl_2 under room temperature and 77 K. No ESR signal is observed for the neutral corroles, indicating that these two compounds contain the low spin d^8 Cu(Ⅲ) central ions under the given experimental conditions, but after reduction with diazabicycloundecene (DBU) an intense ESR signal is observed for each compound in frozen CH_2Cl_2 solution at 77 K as illustrated in Fig.4.

These spectra show a four-line hyperfine splitting due to the strong coupling of the unpaired electron of copper with magnetic moments of the Cu nucleus (I= 3/2, $a_{//}^{Cu}$=236 G for [(T*p*-OCH_3PC)$Cu^{Ⅱ}$]$^-$ and 233 G for [(T*o*,*p*-$(OCH_3)_2$PC)$Cu^{Ⅱ}$]$^-$) as well as a nine-line superhyperfine splitting due to interactions with four corrole nitrogen atoms belonging to the corrole macrocycle. This kind superhyperfine is clearly observed in the high-field part of the spectra ($a_{\perp}^{N}$=17.6 G for both compounds). These typical Cu(Ⅱ) ESR spectra have been reported for other singly reduced copper corroles[12,23,27-28].

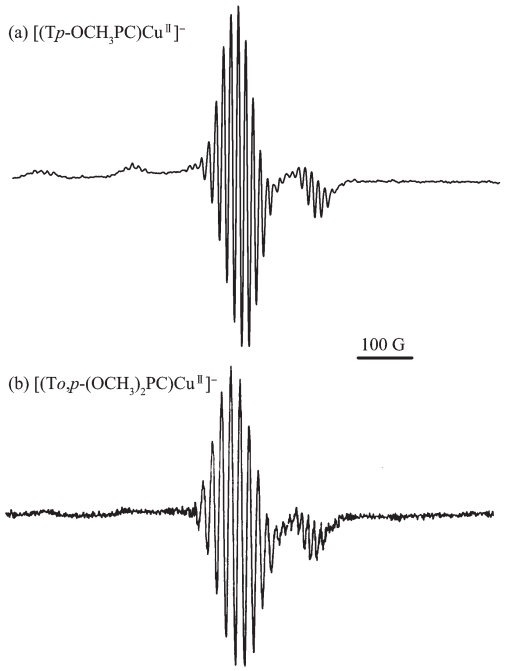

Fig.4　ESR spectra for (a) [T*p*-OCH_3PC)$Cu^{Ⅱ}$]$^-$ (g=2.036) and (b) [T*o*,*p*-$(OCH_3)_2$PC)$Cu^{Ⅱ}$]$^-$ (g=2.037) in CH_2Cl_2 at 77 K

3 Conclusions

Two copper corroles, (T*p*-OCH_3PC)Cu and (T*o*,*p*-$(OCH_3)_2$PC)Cu, were synthesized and characterized by UV-Vis, FTIR, MS, NMR and ESR spectroscopy. Both (T*p*-OCH_3PC)Cu and (T*o*,*p*-$(OCH_3)_2$PC)Cu exist as Cu(Ⅲ) corroles in the solid state and in solutions of CH_2Cl_2 or DMF. An almost identical Soret band is observed in CH_2Cl_2, PhCN, DMF and pyridine, indicating the solvent has only a small effect on UV-Vis spectra of the neutral Cu(Ⅲ) corroles. Effect of the solvent is also weak on macrocycle-centered oxidations, but it is significant on the metal-centered reductions of the corroles. The electron-donating OCH_3 substituents on the *meso*-phenyl rings of the corrole macrocycle can lead to a ~25 nm red-shift of the Soret band and a 60 ~170 mV negative shift of the potentials for the first reduction and first oxidation of (T*p*-OCH_3PC)Cu and (T*o*,*p*-$(OCH_3)_2$PC)Cu as compared to the unsubstituted (TPC)Cu under the same solution conditions.

References:

[1] McGown A J, Badiei Y M, Leeladee P, et al. *Handbook of*

Porphyrin Science: *Vol*.14. Kadish K M, Smith K M, Guilard R, Eds., New York: Academic Press, **2011**:525-599

[2] Aviv-Harel I, Gross Z. *Chem. Eur. J.*, **2009**,**15**:8382-8394

[3] Aviv I, Gross Z. *Chem. Commun.*, **2007**,**20**:1987-1999

[4] Paolesse R. *The Porphyrin Handbook*: *Vol*.2. Kadish K M, Smith K M, Guilard R, Eds., San Diego: Academic Press, **2000**201-232

[5] Erben C, Will S, Kadish K M. *The Porphyrin Handbook*: *Vol*. 2. Kadish K M, Smith K M, Guilard R, Eds., New York: Academic Press, **2000**:233-300

[6] Guilard R, Barbe J M, Stern C, et al. *The Porphyrin Handbook*: *Vol*.18. Kadish K M, Smith K M, Guilard R, Eds., New York: Academic Press, **2003**:303-349

[7] Gao Y, Liu J, Wang M, et al. *Tetrahedron*, **2007**,**63**:1987-1994

[8] Mahammed A, Gross Z. *J. Am. Chem. Soc.*, **2005**,**127**:2883-2387

[9] Mahammed A, Gray H B, Meier-Callahan A E, et al. *J. Am. Chem. Soc.*, **2003**,**125**:1162-1163

[10]Simkhovich L, Luobeznova I, Goldberg I, et al. *Chem. Eur. J.*, **2003**,**9**:201-208

[11]Simkhovich L, Goldberg I, Gross Z. *J. Porphyrins Phthalocyanines*, **2002**,**6**:439-444

[12]Stefanelli M, Mandoj F, Mastroianni M, et al. *Inorg. Chem.*, **2011**,**50**:8281-8292

[13]Pomarico G, Xiao X, Nardis S, et al. *Inorg. Chem.*, **2010**,**49**:5766-5774

[14]Bhattacharya D, Singh P, Sarkar S. *Inorg. Chim. Acta*, **2010**, **363**:4313-4318

[15]Pierloot K, Zhao H, Vancoillie S. *Inorg. Chem.*, **2010**,**49**:10316-10329

[16]Broring M, Brégier F, Burghaus O, et al. *Anorg. Allg. Chem.*, **2010**,**636**:1760-1766

[17]Alemayehu A B, Gonzalez E, Hansen L K, et al. *Inorg. Chem.*, **2009**,**48**:7794-7799

[18]Thomas K E, Wasbotten I H, Ghosh A. *Inorg. Chem.*, **2008**, **47**:10469-10478

[19]Stefanelli M, Mastroianni M, Nardis S, et al. *Inorg. Chem.*, **2007**,**46**:10791-10799

[20]Maes W, Ngo T H, Vanderhaeghen J, et al. *Org. Lett.*, **2007**,**9**:3165-3168

[21]Gryko D T, Tasior M, Peterle T, et al. *J. Porphyrins Phthalocyanines*, **2006**,**10**:1360-1370

[22]Broring M, Brgier F, Tejero E C, et al. *Angew. Chem. Int. Ed.*, **2007**,**46**:445-448

[23]Ou Z, Shao J, Zhao H, et al. *J. Porphyrins Phthalocyanines*, **2004**,**8**:1236-1247

[24]ZHU Wei-Hua(朱卫华), LIAN Cui-Cui(练翠翠), OU Zhong-Ping(欧忠平). *Chemical Reagents* (*Huaxue Shiji*), **2011**,**33**:754-756

[25]Wasbotten I H, Wondimagegn T, Ghosh A. *J. Am. Chem. Soc.*, **2002**,**124**:8104-8116

[26]Zuman P. *Substituent Effects in Organic Polarography*. New York: Plenum Press, **1967**.

[27]Guilard R, Gros C P, Barbe J M, et al. *Inorg. Chem.*, **2004**,**43**:7441-7455

[28]Luobeznova I, Simkhovich L, Goldberg I, et al. *Eur. J. Inorg. Chem.*, **2004**,**43**:1724-1732